

Provolution in the Feature-Optical Beam

Paul Mirsky

paulmirsky633@gmail.com

May 22, 2020

Abstract

In Feature Optics, a light pattern undergoes the process of *provolution* as it propagates; it is analogous to the Fractional Fourier Transform in conventional optics. We study the physical basis of provolution in the simple beam, introducing and incorporating concepts such as imparity, symmetry inclination, and curvature.

1 Introduction

Feature Optics (FO) was recently introduced and elaborated in a series of articles^{1,2,3,4}. FO describes light in terms of its spatial symmetries and asymmetries³, which is useful for modeling diffraction and interference phenomena. Previous work in FO demonstrated its application to beams and gratings^{2,4}. FO is an approximate theory; it sacrifices fidelity both for the sake of simplicity, and to reveal aspects of light that are conventionally overlooked.

FO deals with *patterns*, i.e. functions of intensity vs position, in coherent light. When a plane wave is shaped by an aperture, the transmitted pattern diffracts and changes shape as it propagates. It eventually settles into a stable pattern which remains constant except for overall magnification; this final pattern is the Fourier Transform (FT) of the initial aperture pattern (along with a small residual curvature).

While the FT is usually calculated in a single step, the change of the pattern actually occurs gradually as the light propagates. This process is described by the *Fractional Fourier Transform* (FracFT), which progresses continuously through intermediate *orders*, eventually reaching the ordinary FT. Ozaktas, Mendelovic, and others have produced a large body of work^{5,6,7} describing the FracFT both in purely mathematical terms, and applied to propagating light. They have shown that the FracFT of a pattern 'rides' on a propagating wavefront, which both scales the pattern and imparts a curvature to it.

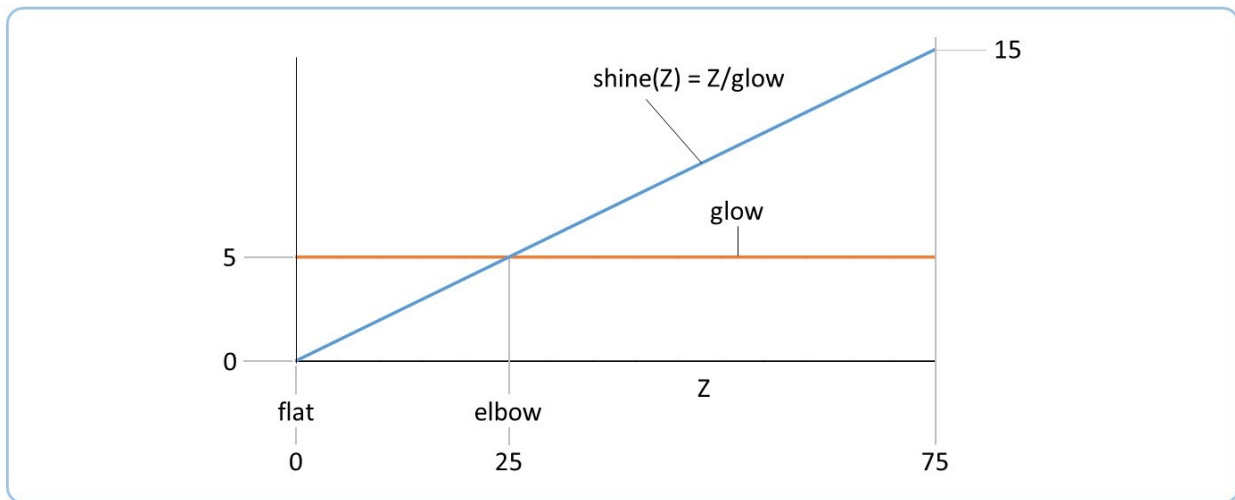
While the FracFT may be applied to any arbitrary pattern, the simplest case is the *Gaussian beam*. This elementary shape describes the simplest transverse mode of the electromagnetic field⁸.

FO describes the same phenomena as conventional wave and beam optics, but uses a different set of concepts and a different physical interpretation. This work ‘translates’ the FracFT of the conventional Gaussian beam into the corresponding concept of *provolution* in FO. This work assumes that the reader is already familiar with theoretical framework developed in earlier work.

2 Glow and shine imparities

Features exist as one of two types: *glow* or *shine*. Glow remains constant during propagation. Shine grows as a linear function of Z , and equals zero where the wavefront is flat. In the simple beam, the glow A is equal to the waist width (in patches) and the shine divergence equals $1/A$. Figure 2.1 shows an example.

Figure 2.1, Glow and shine



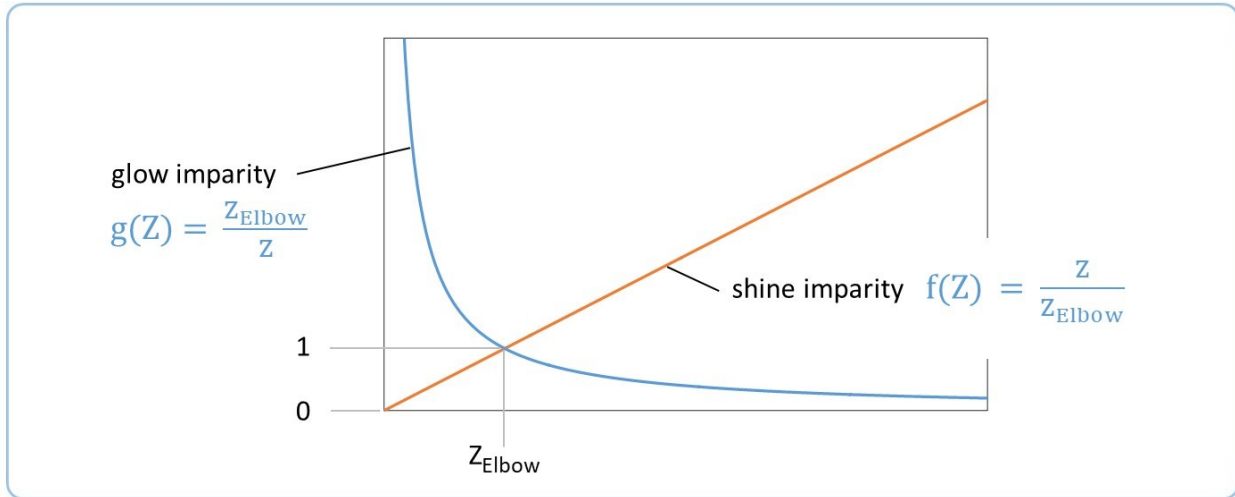
We now consider two different ratios between glow and shine: the *shine imparity* $f(Z)$ and the *glow imparity* $g(Z)$.

$$f(Z) = \frac{\text{shine}(Z)}{\text{glow}} = \frac{Z}{\text{glow}^2} = \frac{Z}{Z_{\text{Elbow}}} \quad (\text{shine imparity})$$

$$g(Z) = \frac{\text{glow}}{\text{shine}(Z)} = \frac{\text{glow}^2}{Z} = \frac{Z_{\text{Elbow}}}{Z} \quad (\text{glow imparity})$$

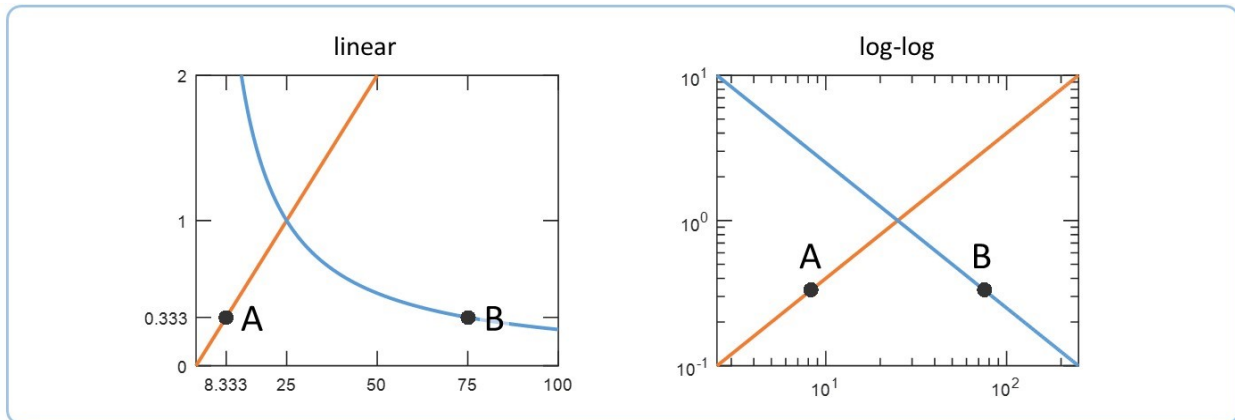
Fundamentally, these two functions are a single degree of freedom; each is simply the reciprocal of the another. As Figure 2.2 shows, the shine imparity begins at 0 at the flat, rises to 1 at the elbow, and increases indefinitely thereafter. The glow imparity begins at infinity at the flat, falls to 1 at the elbow, and approaches zero asymptotically. The two functions coincide at 1 at the elbow.

Figure 2.2, Glow imparity and shine imparity



When the imparities are drawn on a log-log plot, they assume a particularly simple form. Figure 2.3 shows that both glow and shine imparities appear as straight lines, forming an 'X'. The two imparities appear symmetrical around the elbow. The logarithmic symmetry is best seen by comparing the highlighted points A and B which are located at $Z_{\text{Elbow}}/3$ and $3 \cdot Z_{\text{Elbow}}$, respectively. While they are at different distances from the elbow (visible in the linear plot), they differ from the elbow by the same *factor* (which appears as distance in the log-log plot). This factor determines the two points' common imparity of $1/3$. Stated another way, the shine imparity at point A is equal to the glow imparity at point B.

Figure 2.3, Points of equal imparity



3 Inclination as imparity

3.1 Gaussian beam Gouy phase, Fractional FT

The wavefronts of an ideal plane wave are spaced exactly λ apart in Z . However, the wavefronts of a Gaussian beam are displaced from their ideal planes; this discrepancy is called the *Gouy phase*. When the beam waist is located at $Z = 0$, and with Z_R denoting the Rayleigh range,

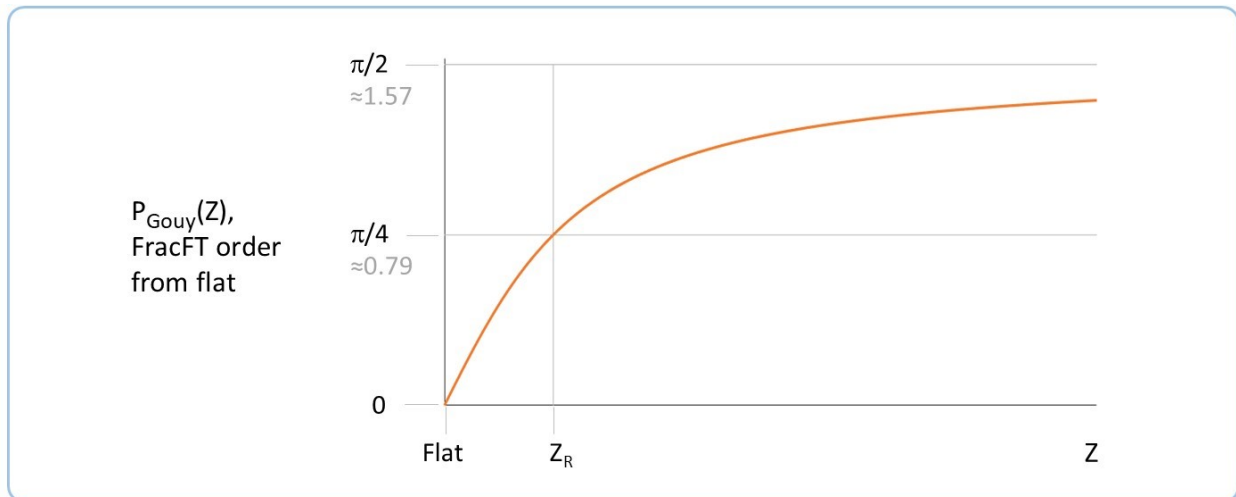
$$P_{\text{Gouy}}(Z) = \arctan(Z / Z_R)$$

For a Gaussian beam, the *change* in Gouy phase between any two planes is also the FracFT order between those planes. Any arbitrary plane may be chosen as the starting plane, where FracFT order is set to zero by definition. Often, we count FracFT starting from $Z = 0$, where $P_{\text{Gouy}} = 0$; in this case, the FracFT order simply equals the Gouy phase.

The FracFT deals with the pattern of the light in a transverse (X - Y) plane, rather than any axial (Z) displacement; so, the definition of Gouy phase given above does not give a clear physical interpretation of the FracFT. Nonetheless, that is how FracFT is quantified in the Gaussian beam.

Figure 3.1 shows the Gouy phase as a function of Z . At the flat, $P_{\text{Gouy}} = 0$. At the elbow (Rayleigh range), $P_{\text{Gouy}} = \pi/4$. The full FT occurs when $P_{\text{Gouy}} = \pi/2$; however, the beam approaches this level only asymptotically.

Figure 3.1, Gouy phase and FracFT order in the Gaussian beam



3.2 Inclination in the Feature-Optical beam

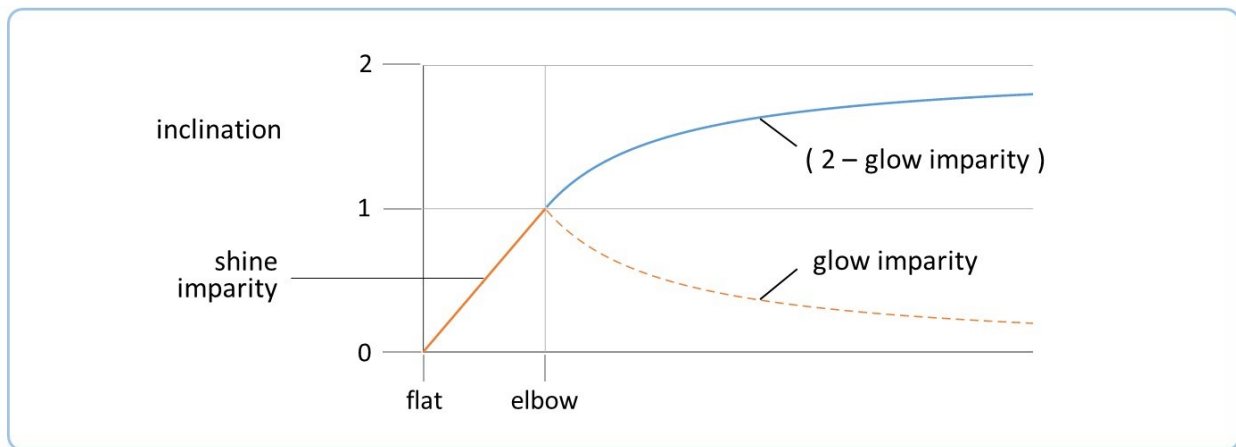
In mathematical terms a pattern is represented by a state vector, which points in some direction or *inclination* in a complex vector space. The FT is a unitary transformation, which rotates the

vector to a different inclination. It also has a rough spatial interpretation, as a later section will describe.

Inclination in FO acts as a parallel concept to Gouy phase in conventional optics – not in the sense of an axial shift of the wavefront, but rather in the sense of the light’s ‘location’ in the progress of provolution. The light provolves from one inclination, to another.

Inclination in the beam is closely related to imparity, as Figure 3.2 shows. It is formed piecewise from two segments, drawn in red and blue respectively. In the first segment, the inclination is equal to the shine imparity, rising from 0 at the flat to 1 at the elbow.

Figure 3.2, Inclination as a piecewise function



In the second segment, it is easier to speak in terms of provolution, i.e. change in inclination. Here, the beam provolves with changes of *glow* imparity. The changes have the same magnitude, but are rectified; i.e., the sense of change is flipped, so that inclination *rises* as glow imparity *falls*. As a result, the inclination after the elbow resembles the glow imparity, reflected across a horizontal line passing through 1. As the glow imparity asymptotically approaches 0 at infinite Z, the inclination asymptotically approaches its final value of 2, which represents a complete FT from the flat.

The inclination can be expressed as

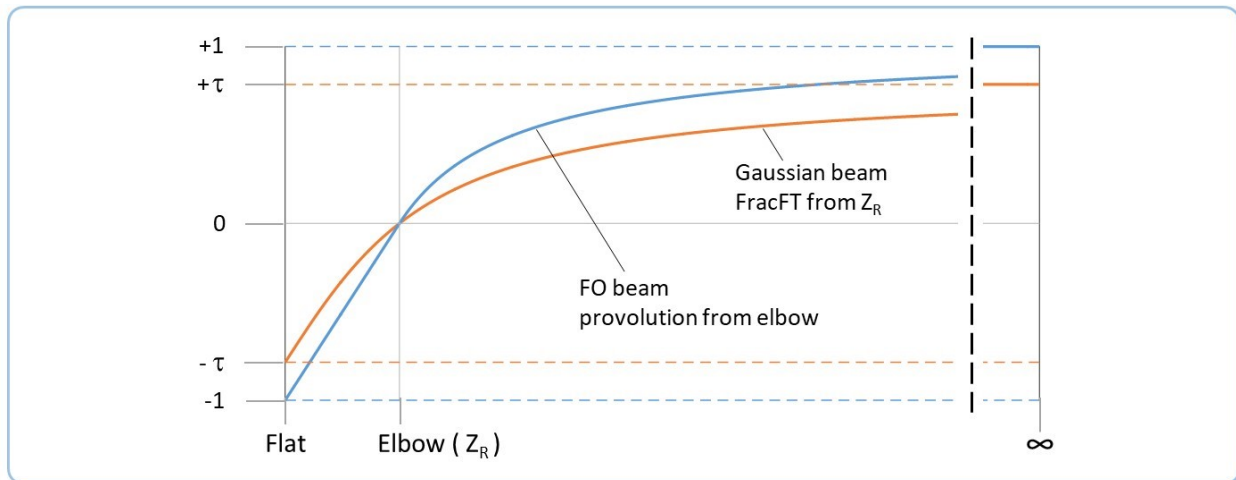
$$i(Z)_{\text{pre-elbow}} = f(Z)$$

$$i(Z)_{\text{post-elbow}} = 2 - g(Z)$$

Figure 3.3 shows the fidelity of the agreement between the Gaussian and FO models. To facilitate the comparison, we have offset the vertical scale by plotting provolution relative to the elbow, rather than inclination per se (which is provolution relative to the flat). Both at $Z = 0$ and (asymptotically) at $Z = \infty$, the two functions have the same slope. However, the FO provolution

at those extremes is greater than the Gaussian FracFT by the Gaussian correction factor τ , which has the value $\pi/4$ and appears as a discrepancy in many similar approximations in FO. Because of this factor, 8 radians corresponds to a complete cycle in FO, rather than 2π radians.

Figure 3.3, Comparing Gaussian and FO models



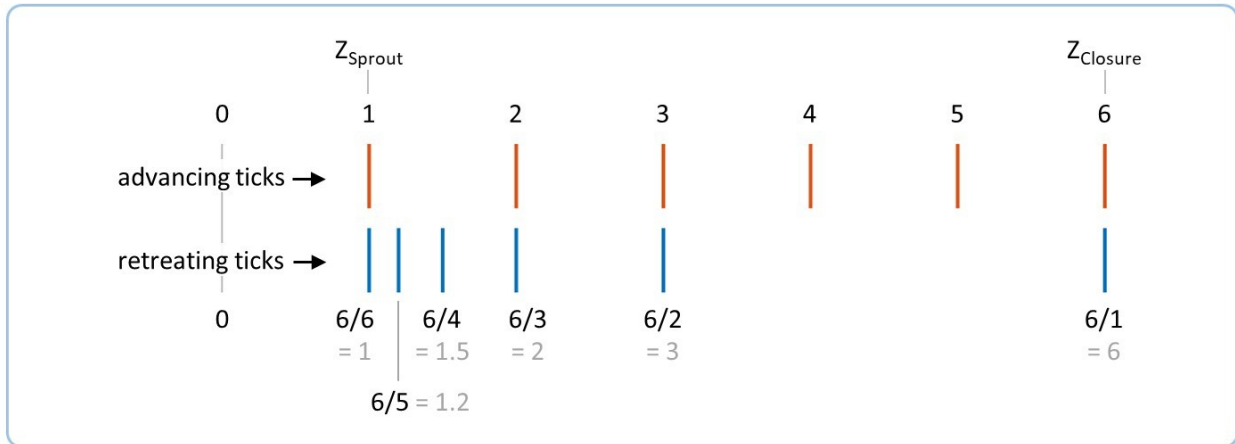
3.3 Ticks

Provolution can be counted by evenly-spaced *ticks*. Each tick corresponds to one patch.

When a new feature sprouts, at some distance Z_{sprout} from the flat, it is 1 patch in size by definition. At distances $2 \cdot Z_{\text{sprout}}$, $3 \cdot Z_{\text{sprout}}$, etc. the feature grows to 2 patches, 3 patches, etc. in a linear fashion. Finally the feature grows to some finite size N where it reaches *closure* and remains indefinitely. Then a new feature sprouts, and the cycle continues.

The sprouting and subsequent closure of a feature defines two sets of planes, as drawn in Figure 3.4. The planes at integer multiples of Z_{sprout} are the *advancing* ticks. The *retreating* ticks occur at inverse-integer fractions of Z_{closure} . There are the same number of advancing and retreating ticks, and both sets always include the sprouting and closure planes, and sometimes some intermediate planes. But, only one set corresponds to even ticks of provolution.

Figure 3.4, Two kinds of ticks



The plane locations are defined by

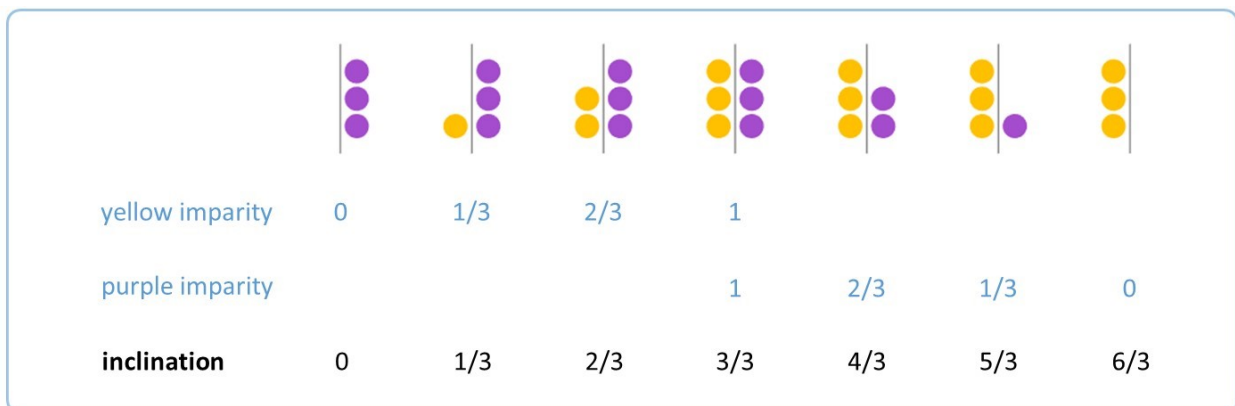
$$Z_{\text{advancing}} = Z_{\text{sprout}} \cdot n, \quad n \in \{ 0, 1, 2, \dots, N \}$$

$$Z_{\text{retreating}} = \frac{Z_{\text{sprout}} \cdot N}{n}, \quad n \in \{ N, (N-1), (N-2), \dots, 2, 1, 0 \}$$

When $n = 0$, imparity is 0. For advancing ticks this occurs at the flat; for retreating ticks, this theoretically occurs at infinity. Each growing feature has its own two sets of planes, but all features share the flat and infinity.

Glow remains constant while shine increases; but, the logic of ticks and imparity is more easily understood if we imagine a counterfactual system in which both shine and glow can change. This is drawn in Figure 3.5, which uses yellow and purple to stand for different types of features; it does not matter which is glow and which is shine. In this system, the yellow feature begins at size 0, then grows to size 3, which is the size of the purple feature. Then, the purple feature decreases from 3 to 0.

Figure 3.5, Ticks by growing and shrinking features



One tick of inclination occurs each time a patch is added to or subtracted from the numerator of the imparity, while the denominator remains constant.

In the actual physical process in the beam far field, imparity decreases because of an increasing denominator, i.e. increasing shine. In physical terms, the glow (the numerator) remains constant. But the retreating ticks occur at the glow-to-shine ratios that *would* correspond to the glow shrinking by one patch after another.

3.4 Ticks in the beam

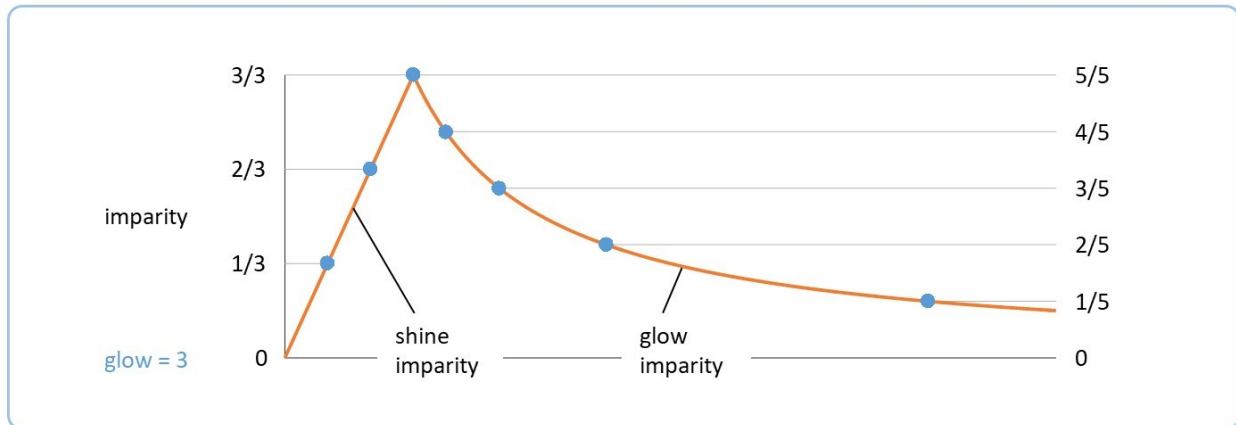
The beam provolves in two stages. As Figure 3.6 shows, the near field provolves by advancing ticks, while the far field provolves by retreating ticks.

Figure 3.6, Two stages of ticks in the beam



The imparities at these ticks are shown in Figure 3.7. Because the glow equals 3, the shine imparity rises from 0 to 1 in 3 ticks of $1/3$ each. The glow imparity falls from 1 to 0 in 5 ticks of $1/5$ each; however, only 4 ticks occur in the finite space shown. The final tick is calculated to occur at infinity, and is never realized.

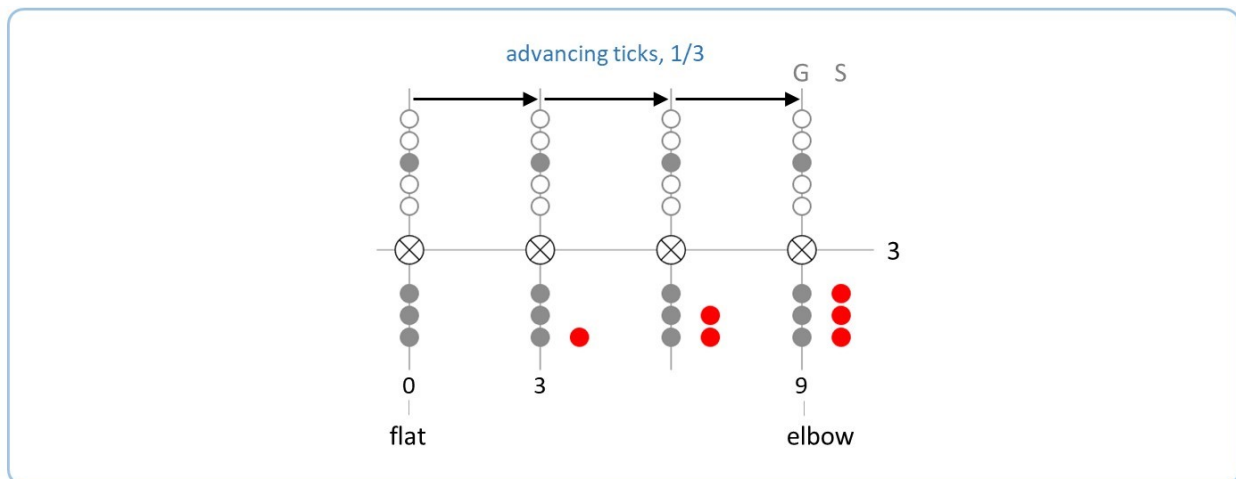
Figure 3.7, Imparity in the beam



It is not possible to observe ticks in the beam. It *is* possible to observe ticks in the revivals of the grating; however, these lie beyond the scope of this work.

The logic of ticks in the beam is best shown using feature diagrams. Note that in this section's diagrams, left and right columns represent glow and shine, respectively; the two columns in later sections will have a different interpretation. Figure 3.8 shows the beam near-field. One advancing tick occurs with the growth of each additional patch of shine. Each tick is a provolution of $1/A$, where A is the glow.

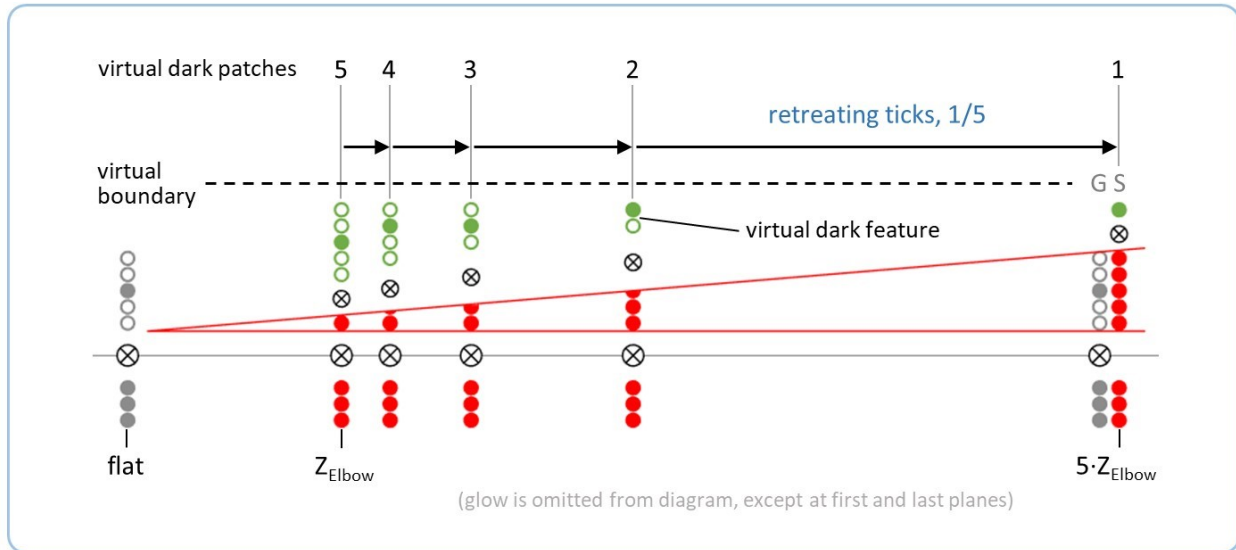
Figure 3.8, Ticks in feature diagram, near field



After the elbow, shine patches continue to grow linearly with Z , with the highest-ranking shine now ranking with dark glow. However, these patches do *not* represent even ticks of provolution. Instead, we must represent the provolution as shown in Figure 3.9. We first imagine a *virtual boundary* to the space, even though there may be no physical boundary present. Then, in each plane we calculate the size of a virtual dark feature (drawn in green) which represents the void between the bright shine and the virtual boundary. Now, one retreating tick occurs with each *decreasing* patch of the virtual dark feature. Note that the Z values and the number of bright

patches at retreating ticks are not always integers. Also, the retreating ticks are bunched near the elbow, and grow further apart.

Figure 3.9, Ticks in feature diagram, far field



The virtual boundary can be set arbitrarily, and this choice affects the ticks' Z locations (but not the shape of the imparity-vs-Z curve). So, the virtual dark shine is a kind of counting trick, not the actual physical cause of the beam's provolution. The real cause is the falling glow imparity. However, they are mathematically equivalent, because both vary in inverse proportion to the growing bright shine.

4 Slab and wedge, width and depth

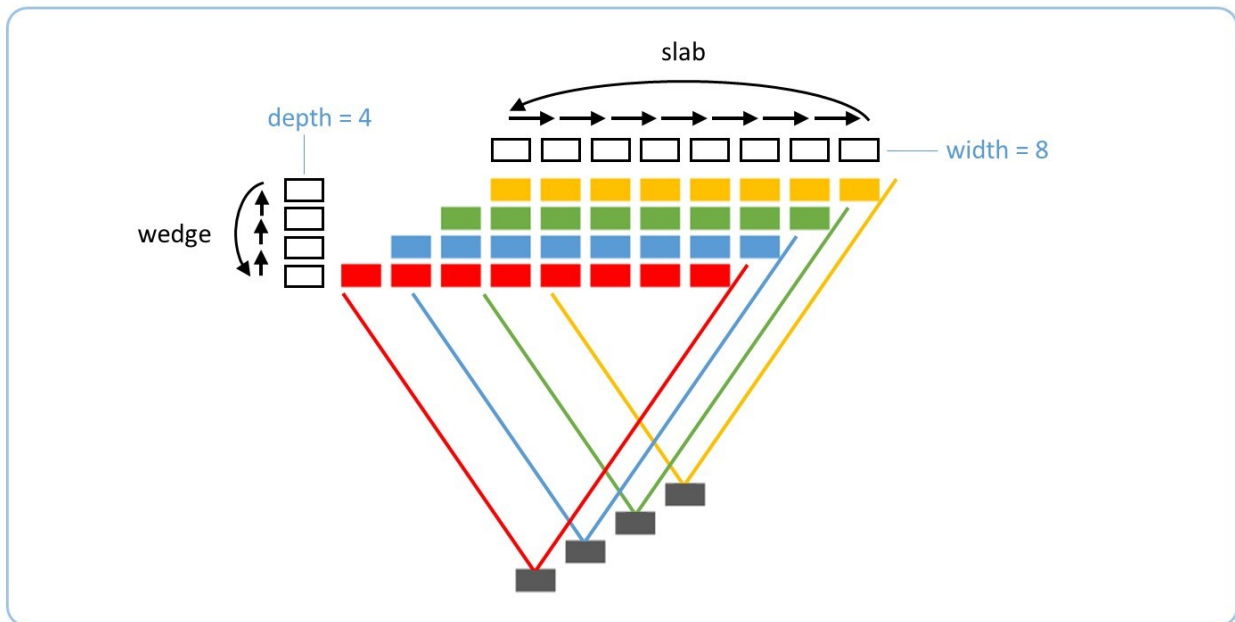
In an earlier work³, we discussed the *slab* and *wedge* transforms. These are defined mathematically as matrices which act on dark and bright state vectors, but they are more intuitively understood as glass optical devices acting on rays, as shown in Figure 4.1. In the cases shown in the figure, slab and wedge act as *asymmetry* transforms, i.e. changing the light from one state to another. However, when the same transforms are applied to certain patterns, they can also act as *symmetry* transforms which leave the state of the light the same, apart from a phase factor applied to the pattern's state vector, which can be thought of as a trivial change.

Figure 4.1, Slab and wedge generators



Figure 4.2 shows a tracked-shine diagram of a simple beam, similar to those drawn in reference 4. This example has a width of 8 patches and a depth of 4 patches, for a total of 32 spatial patches, all of which have the same quantity of energy. Naively, we interpret these numbers as sizes or lengths. But now we add a second, subtly different physical interpretation – namely, how many *symmetries* the pattern has, i.e. the order of its symmetry group. A symmetry generator is a transformation that replaces the energy of each spatial patch with indistinguishable energy from a different patch, such that the end result is entirely equivalent.

Figure 4.2, Slab and wedge in the tracked-shine diagram

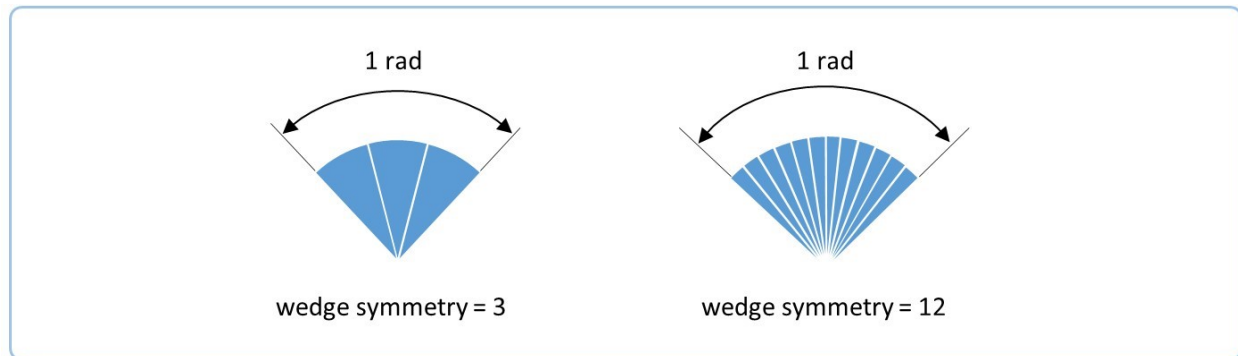


Slab is the symmetry generator corresponding to width. This is very intuitive – an optical slab shifts light laterally, and the width is the number of patches arrayed laterally in the plane, so a slab shifts each patch to the next (we imagine that the final patch is circled around to the first).

Less obviously, wedge is the symmetry generator corresponding to depth. Fundamentally, wedge symmetry is angular rather than translational. It is analogous to the number of sides in a polygon, except that the total angle to be divided among the sides is 1 radian rather than a

complete circle, as Figure 4.3 depicts. The symmetry is not the total angle, which is fixed at 1 radian; the symmetry is also not the angle of each section, though it is related by inverse. Rather, the symmetry is the degree of repetition – how many distinct but equivalent angles the light is spread over.

Figure 4.3, Wedge symmetry



Another way to understand wedge symmetry is as the number of source patches which emanate and shine to a given target patch. Different sources are necessarily at different angles to the target; an optical wedge transforms the angle of each source patch to the next. In fact, a wedge applied in the target plane is equivalent to a slab applied in the source plane.

5 Inclination as symmetry type

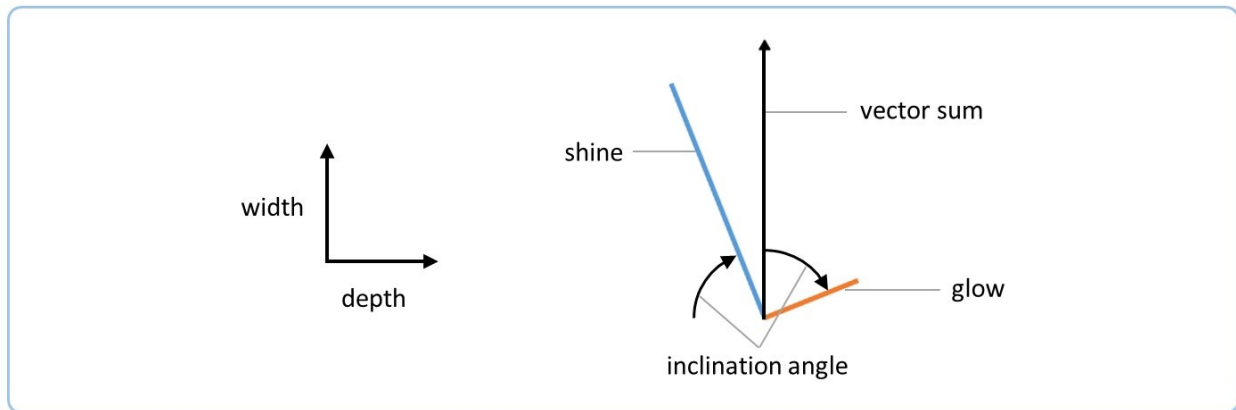
5.1 Gaussian beam inclination

Above, we stated earlier that the inclination can be interpreted as an angle in an abstract vector space. In this section, we interpret the inclination angle as the *symmetry type* of the glow and shine features – whether a given feature has slab symmetry, wedge symmetry, or something intermediate. Equivalently, the inclination of a feature can range from width to depth.

Conventional optics does not include concepts of width and depth. So, here we posit a set of axioms, and study their consequences in the Gaussian beam. In the subsequent section, we adapt the results to the simple beam in FO.

First, we define a plane whose coordinates consist of two orthogonal inclinations: width and depth, shown in Figure 5.1.

Figure 5.1, Inclination concepts in Gaussian beam



Second, we posit that we can represent the glow and shine as two vectors in the plane, with lengths proportional to their respective values.

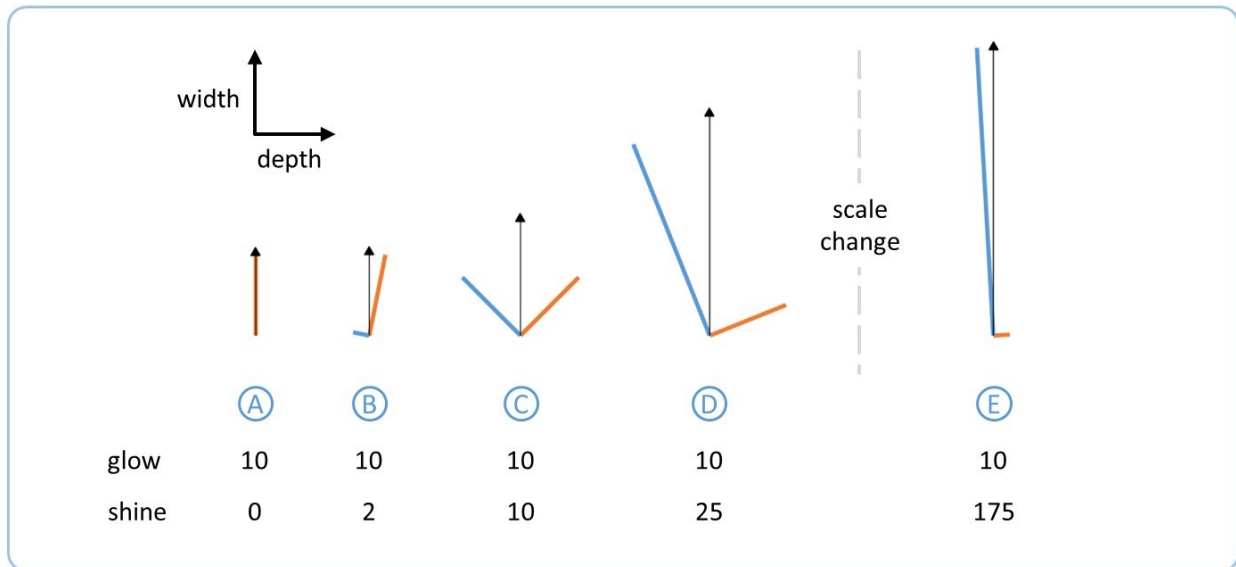
Third, we posit that the vectors are constrained to lie orthogonal to one another.

Fourth, we posit that the *vector sum* of the two vectors is constrained to be wide, while the directions of the glow and shine vectors vary to accommodate the other constraints.

Finally, we interpret the directions of the glow and shine vectors to mean the inclinations of their respective symmetries. Inclination can be quantified in either of two equivalent ways: the angular distance from width to glow, or the angular distance from depth to shine.

From these assumptions we find the behavior shown in Figure 5.2, which tracks the inclinations as the shine grows from 0 to very large, while the glow remains at constant magnitude. At the waist in Figure 5.2a, the shine is 0 and the glow is purely wide. In Figure 5.2b, the first shine appears. Because the shine is much smaller than the glow, the vector sum deviates only slightly from the glow. The vector sum is constrained to be wide, and the shine is constrained to be orthogonal to the glow; therefore, the shine is nearly deep (with a slight deviation).

Figure 5.2, Width and depth vs shine growth



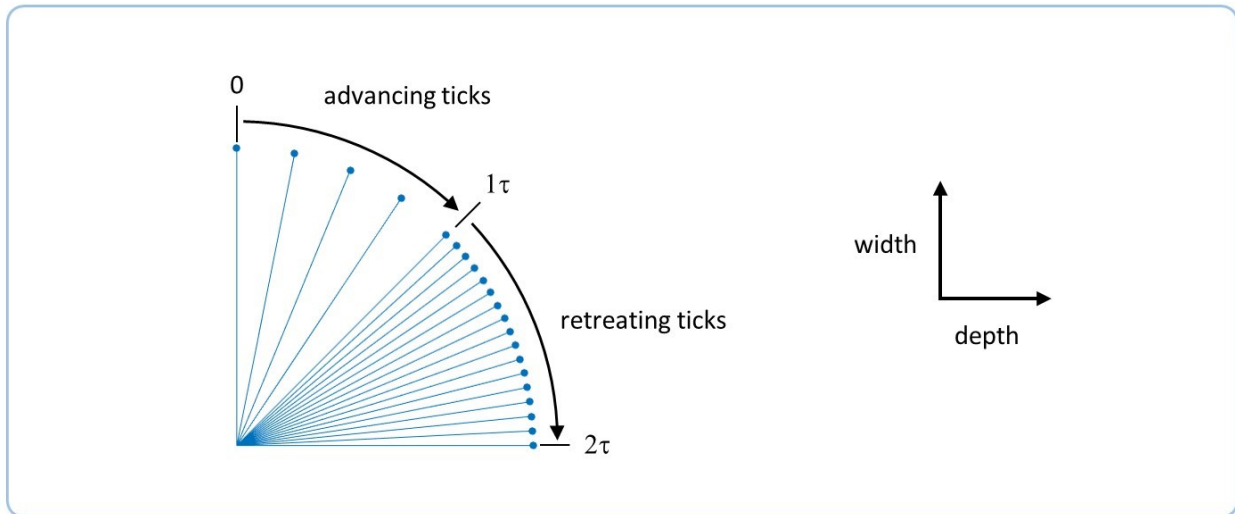
As the shine grows, the angles of both glow and shine tilt. By the elbow in Figure 5.2c, the two vectors are of equal magnitude and both symmetries incline intermediately between width and depth. Beyond the elbow, the shine tilts further and further towards width while the glow tilts further and further towards depth, approaching those inclinations asymptotically as shine grows infinitely large.

In summary, the effect of the provolution is that the glow tilts from width to depth, and the shine tilts from depth to width. They are coupled together, and turn as a single unit. Note that we consider the shine at the flat to be deep because the first patches to sprout are deep, even though the shine inclination at the flat is actually undefined because its magnitude is zero.

5.2 Inclination by ticks in FO

The conclusions of the previous section can also be applied to the FO beam, with only small adjustments. Inclination in the FO beam can be converted to angle by simply multiplying by the Gaussian correction factor τ . Figure 5.3 shows how advancing (near-field) and retreating (far-field) ticks can be interpreted as even steps in angle. Note that the inclinations shown in this figure apply to the glow; the shine is inclined perpendicular to the glow.

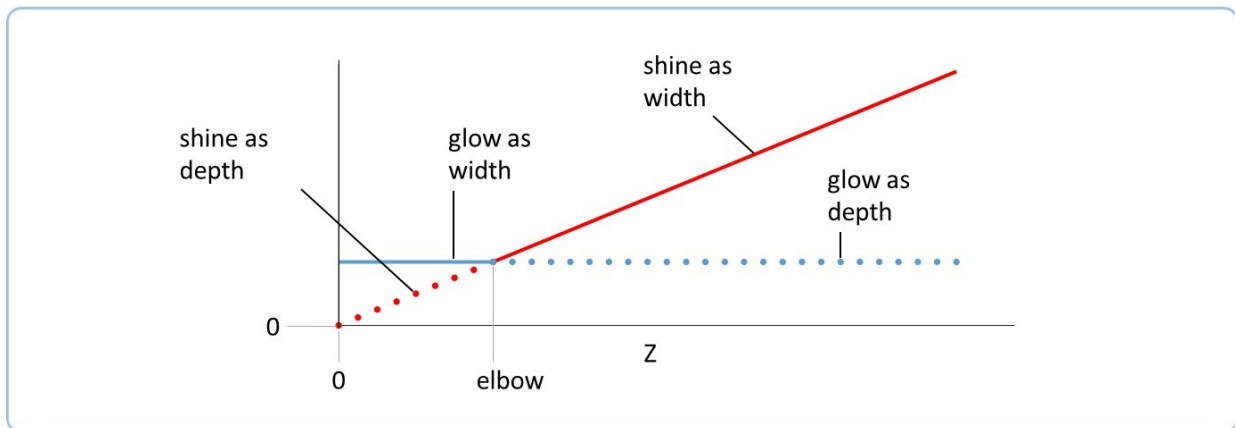
Figure 5.3, Inclination angles



5.3 Inclination in feature diagrams

In the previous section, we allowed inclinations to assume a continuous range from wide to deep. However, feature diagrams are not able to show such a range; instead, a feature can have one of only two discrete inclinations: width, or depth. Therefore, we make the approximation shown in Figure 5.4; solid lines (of either color) represent width, while dotted lines (of either color) represent depth; red represents shine, while blue represents glow.

Figure 5.4, Glow and shine, width and depth



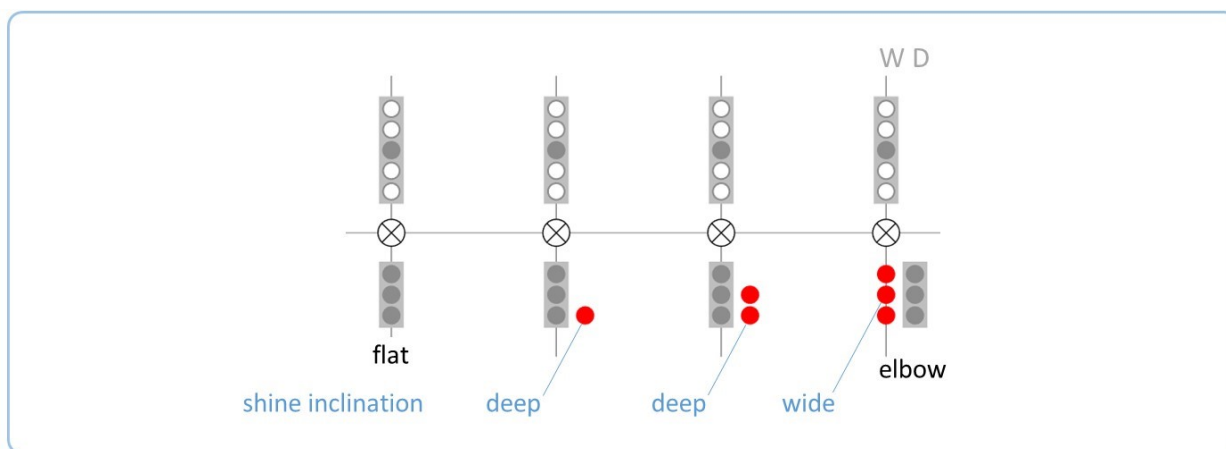
From the flat up to the elbow, the glow is wide while the shine is deep. At the elbow, they abruptly exchange inclinations, which they maintain thereafter. An equivalent statement is that the *larger* of the two is always wide, while the smaller is always deep.

This approximation is very accurate at the flat and near the end field, but its fidelity diminishes near the elbow. Therefore, feature diagrams follow the arbitrary convention of drawing the shine wide at the elbow, although it is actually halfway between wide and deep.

Now we establish new conventions for indicating inclination in feature diagrams. The need for these conventions will become more apparent in future works, where they will be applied to the grating.

Figure 5.5 shows the beam near field. For each plane, there are two columns, labeled 'W' and 'D' for wide and deep. (Note that this convention differs from the one used above in 3.1, as well as in previous work⁴, where the left column always represented glow and the right column always represented shine.) Glow is drawn in dark grey, while shine is drawn in different colors for different features. Glow is also highlighted with a dark background to make its inclination more visible.

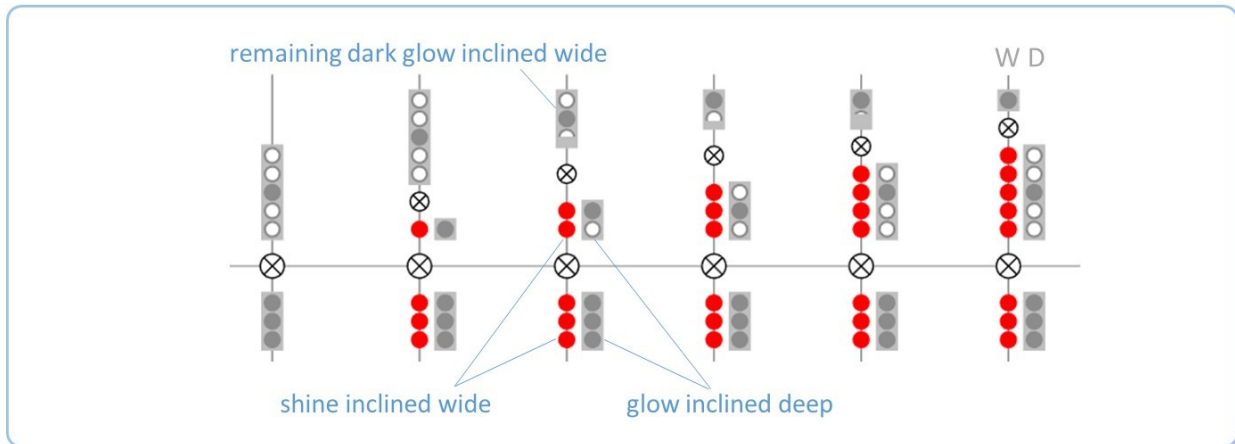
Figure 5.5, Inclination in near field in feature diagram



In the near field, a red feature grows in the depth column, indicating that the shine is inclined deep. At the elbow the lowest-ranked glow and shine switch inclinations, indicated in the diagram by their switching columns.

Figure 5.6 shows the beam in the far field. The available space is represented as dark glow, which works differently from bright glow. Here, the shine immediately grows wide, which tilts the dark glow to depth. As long as the beam propagates, bright shine continues to grow and to tilt an equal amount of dark glow.

Figure 5.6, Inclination in far field in feature diagram



6 Provolution as conjugation

The above discussion has treated the glow and shine similarly to objects which may be rotated from one inclination or angle to another. Mathematically, this may be represented by matrix multiplication. For example, in previous work¹ we described how the Fourier Transform (FT) acts to *transform* a state vector, yielding a new state vector. For example, it turns a bright feature into a dark feature.

$$\text{FT} \left(\frac{1}{\sqrt{3}} \cdot \begin{bmatrix} 1 \\ 1 \\ 1 \end{bmatrix} \right) = \begin{bmatrix} 0 \\ 1 \\ 0 \end{bmatrix}$$

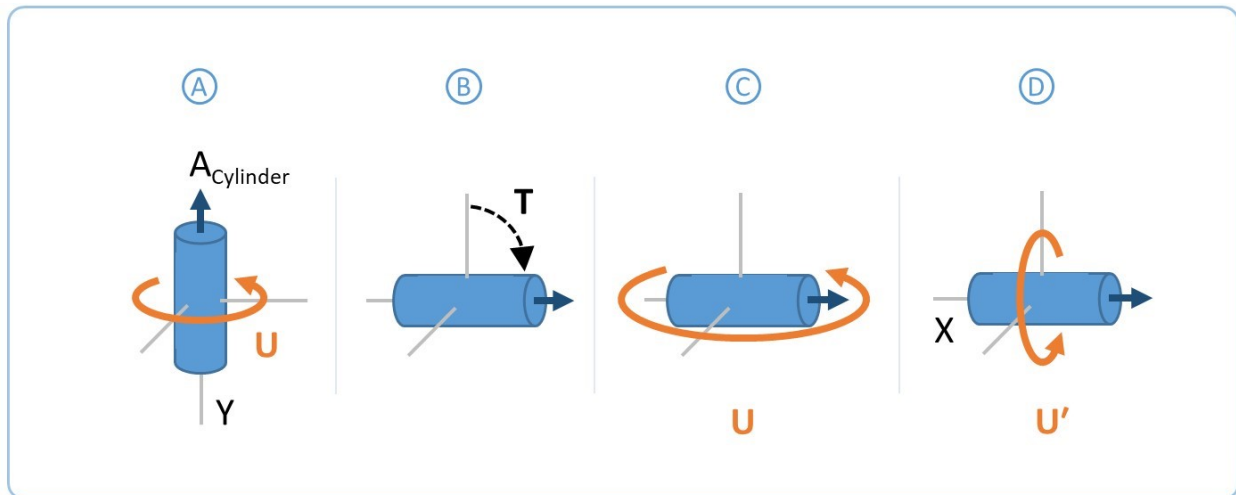
However, the FT matrix acts differently on the *symmetry* of the state vector; namely, it acts by *conjugation*, which is distinct from transformation. Rather than act on a state, conjugation acts on another transformation. In this case, the other transformation belongs to the symmetry subgroup or asymmetry subgroup of the state vector. For instance, the FT conjugates the slab group S into the wedge group W.

$$\text{FT}^{-1} \cdot \text{S} \cdot \text{FT}^{+1} = \text{W}$$

The key principle can be stated as: when a state vector is *transformed* by any transformation T, then its symmetry and asymmetry subgroups are both *conjugated* by T as well.

The concept of conjugation is best visualized through a more intuitive example. As shown in Figure 6.1a, we begin with a cylinder with its axis A_{Cylinder} lying parallel to the vertical axis Y of the fixed coordinate system. The symmetry group U of the cylinder includes all rotations around its symmetry axis A_{Cylinder} . In terms of fixed coordinates, they rotate the cylinder around Y.

Figure 6.1, Conjugation of symmetry



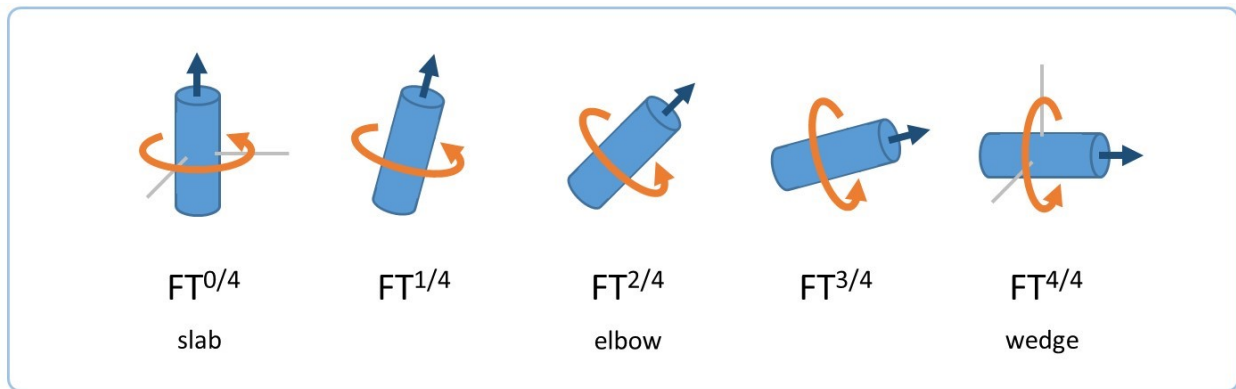
Next as shown in Figure 6.1b, we apply an instantaneous transformation T , which reorients the cylinder by a quarter-turn so that its axis A_{Cylinder} lies horizontal.

We contrast two possibilities for what happens to the symmetry group U , depending on whether we understand U to be defined relative to the fixed coordinate system, or relative to the cylinder's own coordinates. If U remains fixed, then it continues to rotate around Y . Then, its effect post- T is to flop the cylinder end-over-end as shown in Figure 6.1c. In this case, U is no longer a symmetry, but rather an *asymmetry* group.

On the other hand, if we imagine that U 'travels' with the cylinder itself, then we conjugate U by transformation T , resulting in group U' , which consists of rotations around the horizontal axis X . U' is a similar set of transformations to U , but they are performed from a different perspective. U' continues to rotate the cylinder around A_{Cylinder} , as shown in Figure 6.1d, making it a symmetry group.

While the previous figure shows only the endpoints of transformation T , Figure 6.2 shows the provolution as a series of many gradual steps. This better resembles what actually occurs in the FracFT.

Figure 6.2, Gradual change of inclination



In FO, a provolution of 2 (i.e., the full FT) conjugates slab symmetry into wedge symmetry and vice-versa. While these are all transformations, there is a great physical difference between the provolution and the symmetry transformations. To clarify the distinctions:

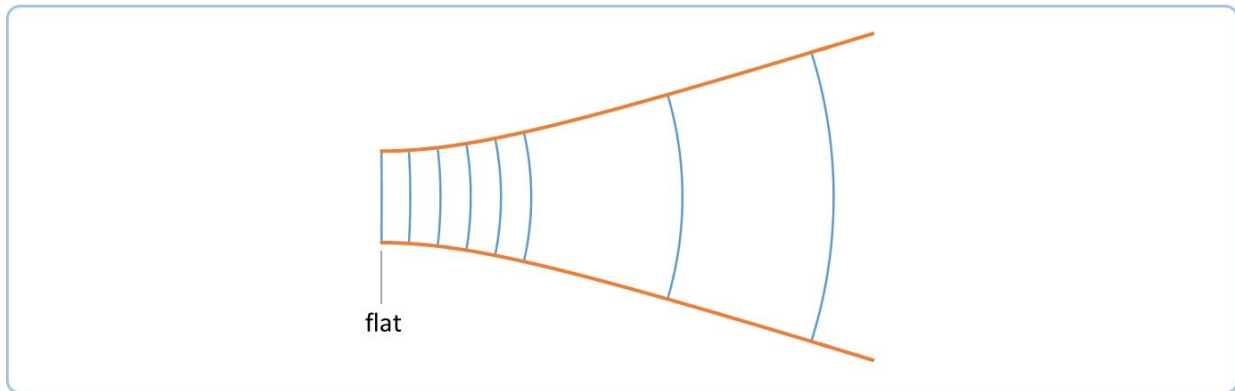
- The symmetry is only a possible or potential transformation; no physical motion actually takes place. The provolution actually does take place.
- The symmetry acts by transformation, while the provolution acts by conjugation.
- The symmetry acts on the state vector of the light, while the provolution acts on the symmetry transformation matrices.
- The symmetry transformation applies within a single plane at a given instant; the provolution occurs from one plane to another over finite time and distance.
- The symmetry does not cause any change in the provolution. However, the provolution does change the symmetry, conjugating it from one inclination to another.
- In the far field, the provolution eventually slows and nearly stops, even as the beam continues to propagate and expand. However, the symmetry persists indefinitely.

7 Curvature

7.1 Gaussian beam curvature

The Gaussian beam is named for its transverse profile, whose intensity has a Gaussian distribution. However, we will be concerned with other properties of the beam and how they vary along the propagation axis Z , not along the transverse axis. The beam has a flat wavefront at the waist, but in any other plane the wavefront is curved like a portion of a notional sphere, as shown in Figure 7.1.

Figure 7.1, Curved wavefronts in the Gaussian beam



This radius of curvature varies with propagation in Z following the equation

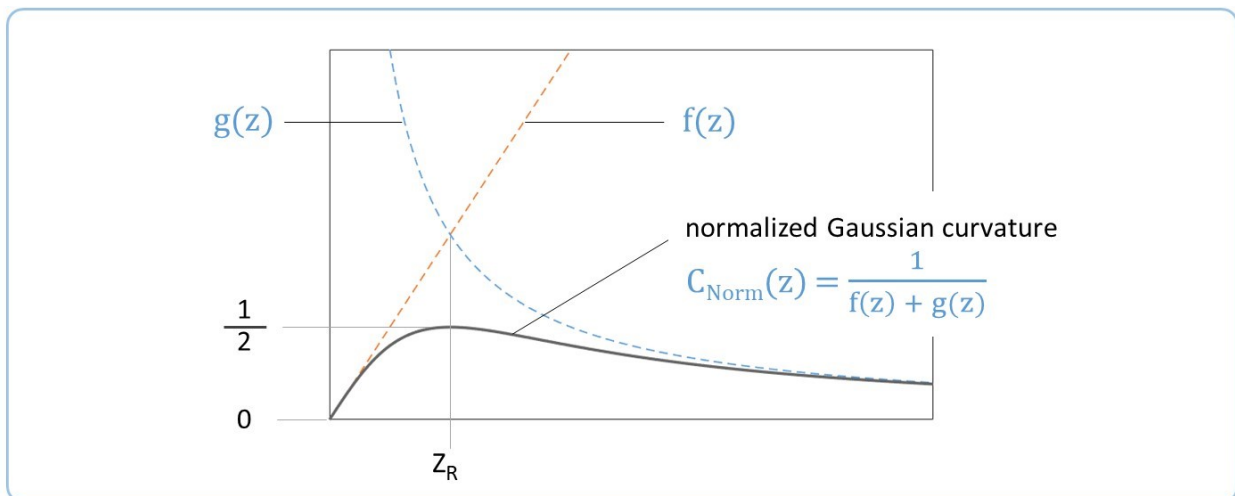
$$R(Z) = Z \cdot \left[1 + \left(\frac{Z_R}{Z} \right)^2 \right]$$

Alternatively, the *normalized curvature* – i.e. the actual curvature, multiplied by Z_R – is equal to the reciprocal of the sum of the glow and shine imparities.

$$C_{\text{Norm,Gaussian}}(Z) = \frac{1}{f(Z) + g(Z)}$$

$C_{\text{Norm,Gaussian}}$ is drawn in Figure 7.2. At the flat, it matches the shine imparity. In the far field, it matches the glow imparity. At the Rayleigh range (elbow), it has a rounded peak with a height of $\frac{1}{2}$.

Figure 7.2, Normalized Gaussian curvature



7.2 Piecewise normalized curvature in FO

FO describes curvature using an approximation. Normalized curvature can be expressed as a simple ratio

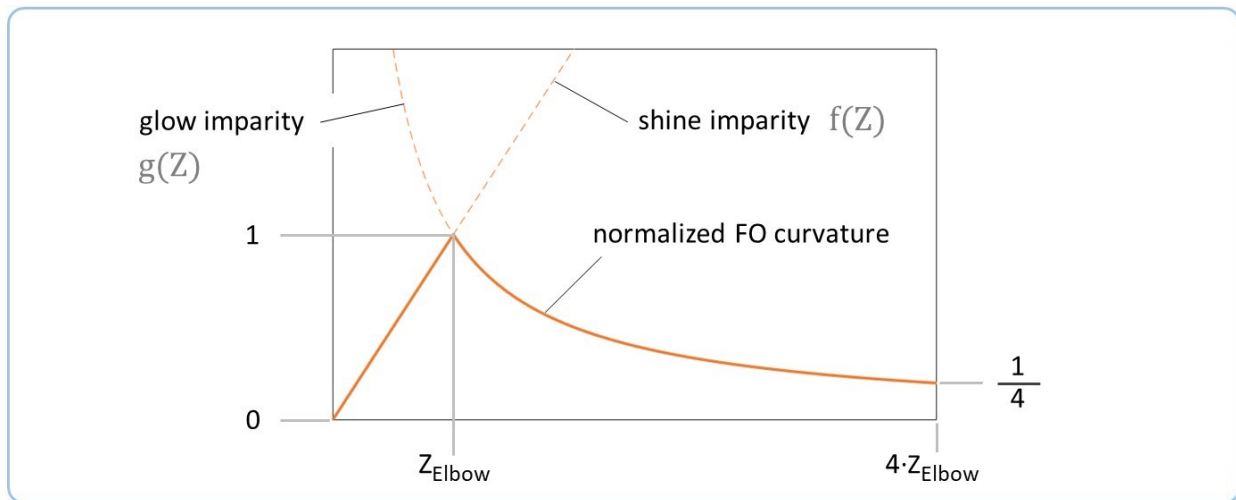
$$C_{\text{Norm,FO}}(Z) = \frac{\text{depth}(Z)}{\text{width}(Z)}$$

Depth and width are piecewise functions made from glow and shine imparities; so, C_{Norm} can be expressed as

$$\begin{aligned} C_{\text{Norm,FO}}(Z) &= f(z) , & Z < Z_{\text{Elbow}} \\ &= g(z) , & Z \geq Z_{\text{Elbow}} \end{aligned}$$

This function is drawn in Figure 7.3. Before the elbow, the curvature rises proportionally to the distance Z ; for example, at $\frac{1}{2} Z_{\text{Elbow}}$, C_{Norm} is $\frac{1}{2}$. After the elbow, the curvature is inversely proportional to Z ; for example, at $4x Z_{\text{Elbow}}$, C_{Norm} is $\frac{1}{4}$. As Z becomes greater and greater, C_{Norm} becomes smaller and smaller.

Figure 7.3, Normalized curvature in FO as a piecewise function



C_{Norm} has a sharp, discontinuous peak at the elbow. The peak height is 1 for all beams, which is twice the rounded peak in the Gaussian curvature.

In terms of actual (non-normalized) curvature

$$C(z) = \frac{z}{\text{glow}^4} , \quad Z < Z_{\text{Elbow}}$$

$$C(z) = \frac{1}{z} , \quad z \geq z_{\text{Elbow}}$$

The second component has the interpretation that in the far field, the wavefronts are formed from portions of a notional sphere whose center lies in the flat plane.

8 The converging beam

8.1 Even and odd parameters

Up to this point, we have assumed that the beam begins at the flat waist. However, a *converging* or focused beam may also exist, as drawn in Figure 8.1. It is typically produced by passing a wide beam through a lens (not drawn); the wavefront leaving the lens has a concave curvature that causes the beam to narrow as it propagates. From the waist onward, it is exactly the same as the beams we have studied up to this point.

Figure 8.1, Converging beam

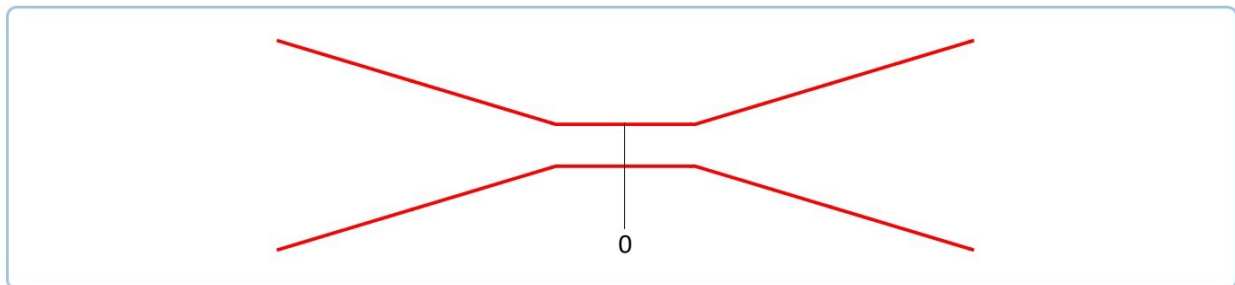
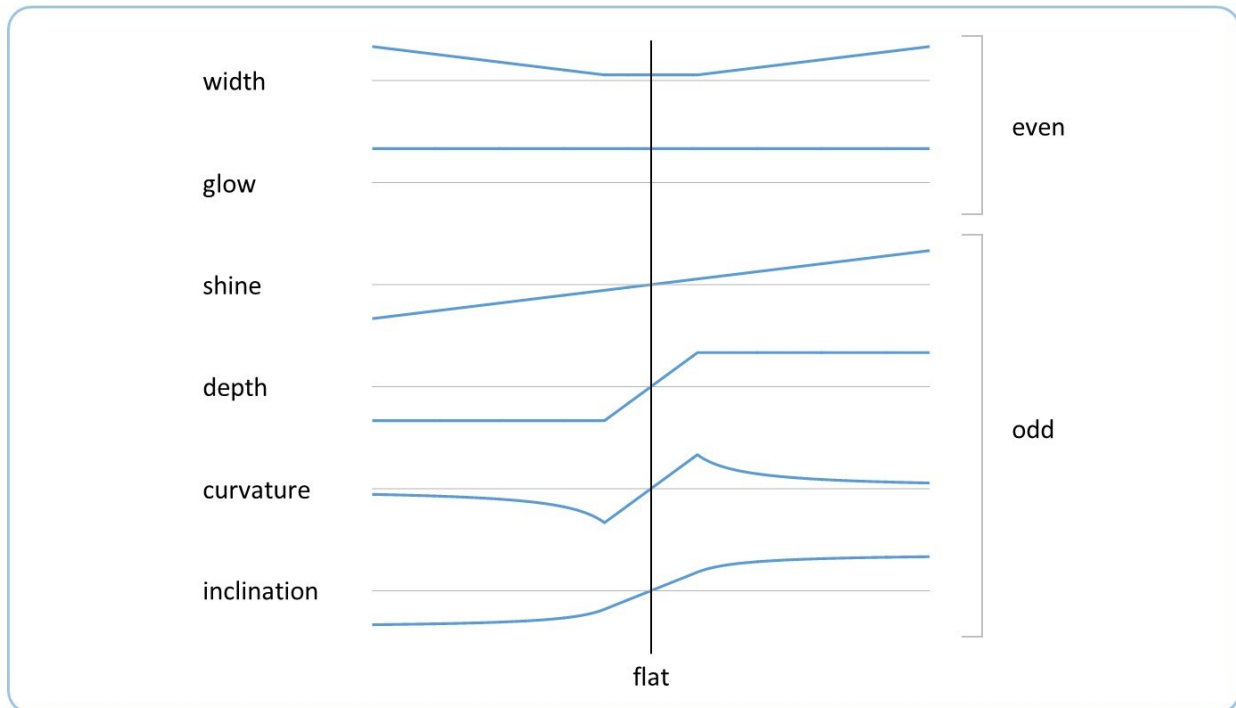


Figure 8.2 shows the variables which describe the beam. All have either even or odd symmetry around the waist, i.e. the value at any negative Z always has the same magnitude as at the corresponding positive Z , but its sign may be flipped.

Figure 8.2, Many variables in converging beam



For a hypothetical converging beam which extends infinitely far in both directions, the total provolution end-to-end equals 4 radians. For a real, finite beam, it is always less than that.

For $Z < 0$, shine is *negative*. The existence of negative shine shows that one must *not* naively interpret increasing shine as something analogous to an expanding gas, for which a negative volume would be impossible. Also, negative shine spontaneously moves towards zero as it propagates, which is the opposite of the behavior of a gas.

While the *magnitude* of negative shine falls as it approaches the waist, and rises afterwards, these are actually two expressions of the same principle. In both cases, the shine value increases in linear proportion to Z , regardless of whether shine is positive or negative. This root principle determines the evolution of the beam shape; other properties such as curvature follow from the shine.

8.2 Provolution across the flat

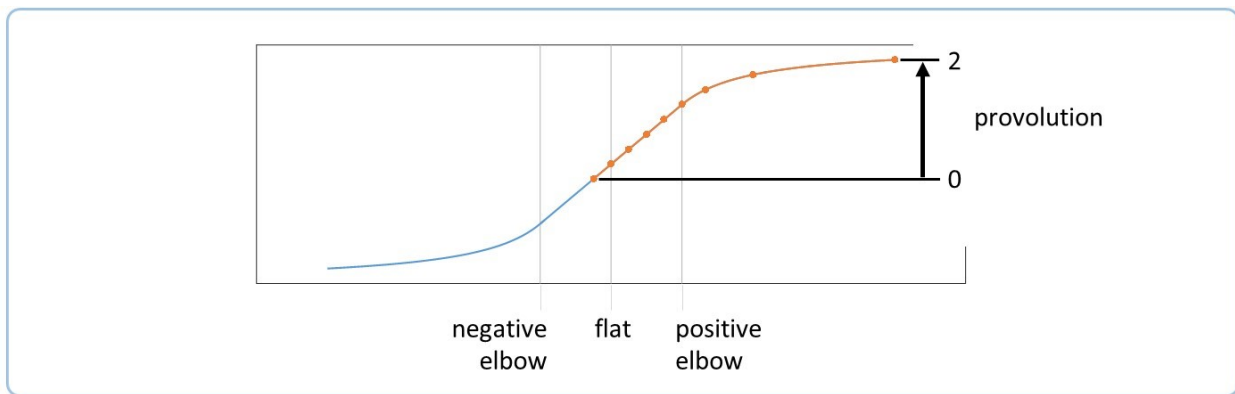
In earlier sections we regarded the flat as the starting point of the beam, and accordingly we assigned the net provolution to be 0 at the flat. In that case, the beam reached the full FT only at infinite Z . But in general, the provolution may be counted from *any* plane, and the FT occurs for any net provolution of 2 radians.

If the flat is taken as the starting plane, then the FT is approached only asymptotically with infinite propagation in Z . If any plane *after* the flat is taken to be the starting plane, then the FT

never occurs and is never approached even asymptotically, as long as the beam propagates freely with no lens. However, if a plane *before* the flat is taken to be the starting plane, then the FT may be reached in finite distance.

In this section, we will consider provolution counted from planes of negative shine, before the flat. Figure 8.3 shows the provolution of a converging beam, counted from one tick before the flat – in this case, a tick of $\frac{1}{4}$ radian. The full FT occurs at $\frac{1}{4}$ radian before the end field, which occurs at $4x$ the positive elbow distance. Rather than provolving by 4 ticks of shine imparity and 4 ticks of glow imparity, the beam provolves by 5 ticks of shine imparity and 3 ticks of glow imparity.

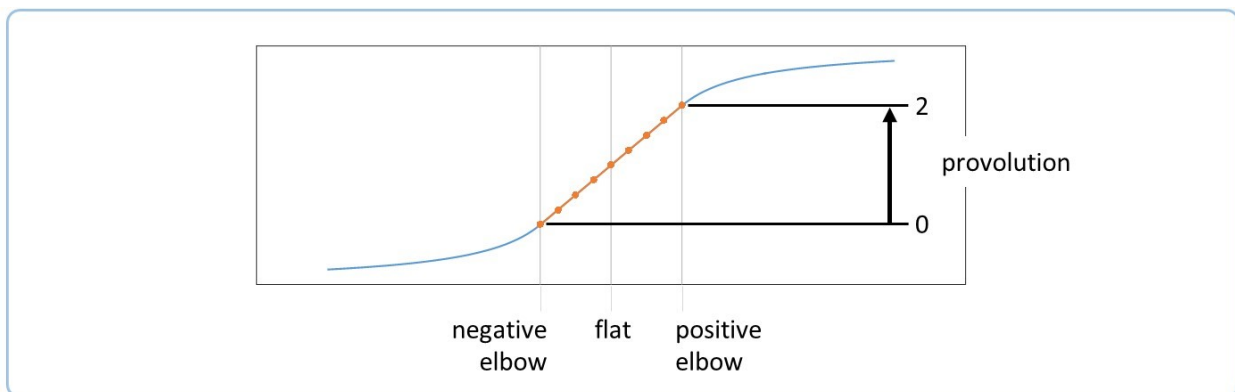
Figure 8.3, Provolution from near flat



Note that to simplify counting by ticks, we are considering the case in which both the bright glow and the available dark glow (which defines the virtual boundary) are of the same size, i.e. 4 patches. However, this is not strictly necessary.

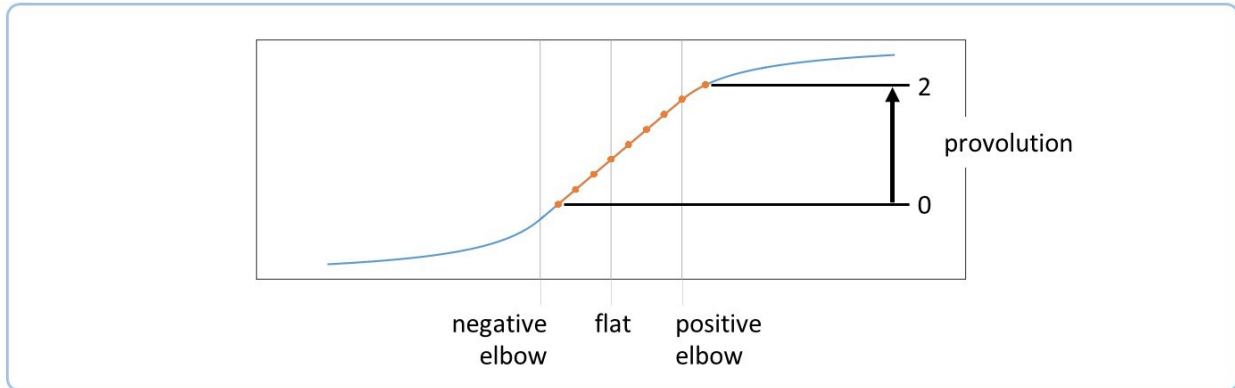
In another example shown in Figure 8.4, the negative elbow is taken as the starting plane. Here, the beam provolves a full 2 radians in a distance of $2 \cdot Z_{\text{Elbow}}$. The provolution proceeds by 8 ticks of shine imparity, each of increment $\frac{1}{4}$ radians. It starts and ends at the same-magnitude imparity.

Figure 8.4, Provolution from elbow



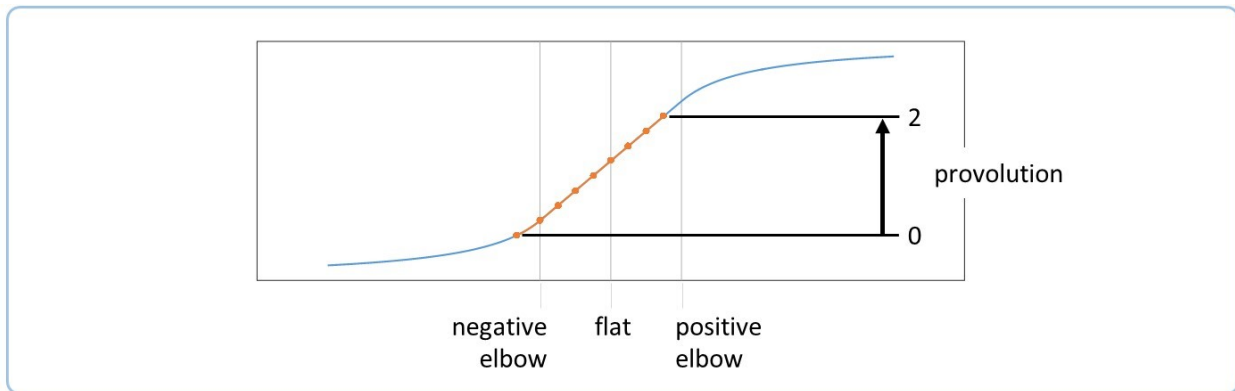
Next we consider the case of a starting plane that falls only slightly after the negative elbow, shown in Figure 8.5. It provolves by 7 ticks of shine imparity and 1 tick of glow imparity.

Figure 8.5, Provolution from near elbow



Finally, note that all of these cases have analogous equivalents in which forward and backward directions are reversed. For example, Figure 8.6 below shows a case that is the reversed case of the previous Figure 8.5.

Figure 8.6, Provolution from near elbow, reversed



9 The lens and flip field

9.1 The lens

Conventionally, the principle of the lens is stated as: the lens causes a step change in the curvature of the beam; the size of this step is equal to the negative inverse of the focal length.

$$C_{\text{out}} = C_{\text{in}} + \Delta_{\text{Lens}}$$

$$\Delta_{\text{Lens}} = -\frac{1}{F_{\text{Lens}}}$$

In FO, in the context of the 2f system, the principle is stated differently: the lens *exchanges* the values of the glow and the shine; also, it flips the sign of the shine from positive to negative.

$$\text{shine}_{\text{Out}} = -1 \cdot \text{glow}_{\text{In}}$$

$$\text{glow}_{\text{Out}} = \text{shine}_{\text{In}}$$

This does not change the width of the light. It also does not change the magnitude of the depth; however, the sign of the depth is flipped.

Note that these relations hold true only when the flat is located in the front focal plane of the lens, as in the standard 2f configuration. Also note that in the context of these equations, the subscripts 'in' and 'out' refer to the front and rear surfaces of the lens, *not* to input and output planes of the 2f system.

Because imparity between glow and shine is defined as the ratio of the smaller to the larger, it remains unaffected when the two values are exchanged. Therefore, the lens changes shine imparity into glow imparity and vice-versa, but leaves the magnitude of the imparity the same.

$$\text{shineImparity}_{\text{Out}} = -1 \cdot \text{glowImparity}_{\text{In}}$$

$$\text{glowImparity}_{\text{Out}} = -1 \cdot \text{shineImparity}_{\text{In}}$$

This abruptly changes inclination by -2 radians. However we do not count this change as a provolution, i.e. it does not count towards the FT.

9.2 The 2f system

A free beam (i.e., no lens) can be parameterized by the width and Z-position of its waist. Accordingly, the lens changes one free beam into another free beam. As Figure 9.1 shows, the beam entering the lens has a waist at the input plane; the beam leaving the lens has a waist in the output plane.

Figure 9.1, Lens changes one beam to another

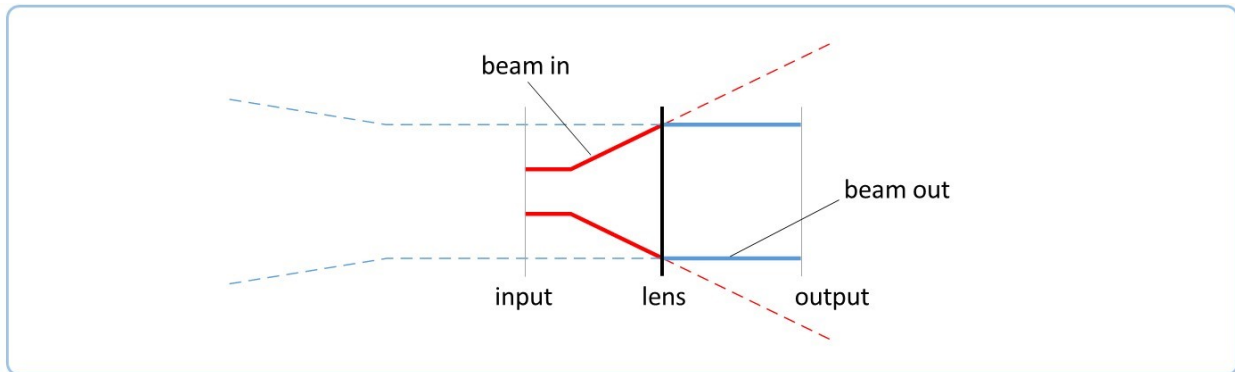
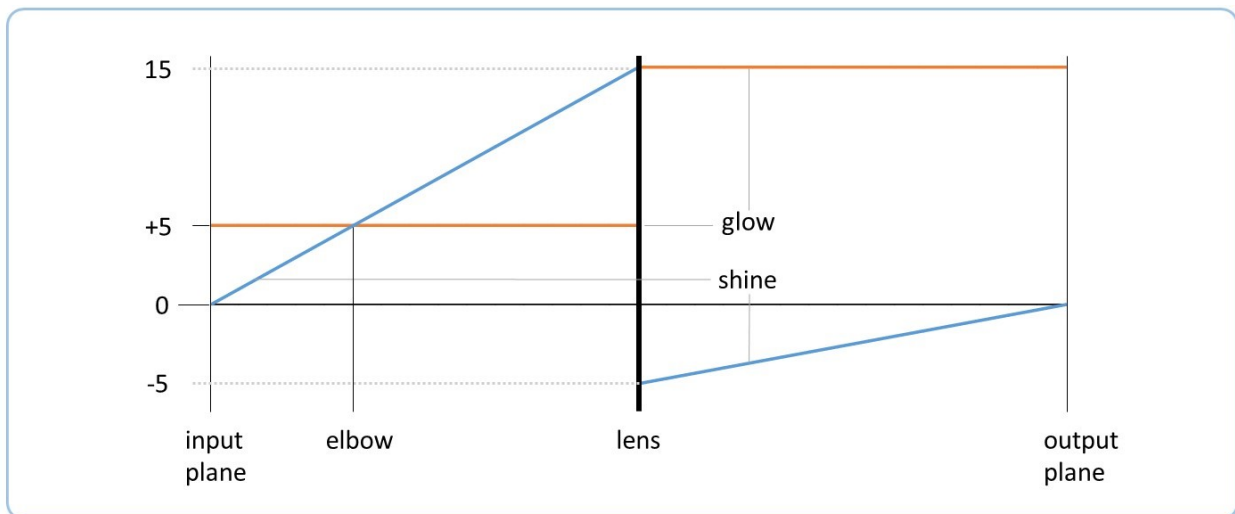


Figure 9.2 illustrates the course of glow and shine in a typical 2f system. The region before the lens is the same as in Figure 2.1; the glow stays constant while the shine increases linearly. The lens then exchanges the glow and shine as described above in section 9.1.

Figure 9.2, Glow and shine in 2f system



In the flip field, the glow remains constant and becomes the final beam width in the output plane. The negative-valued shine increases as it propagates, shrinking in magnitude. Regardless of beam size, the shine reaches zero at the output plane because the divergence angle of the shine is equal to the inverse of the glow⁴.

$$\text{div}_{\text{shine}} = \frac{1}{\text{glow}}$$

Accordingly, for both sides of the lens

$$\text{shine}(Z) \cdot \text{glow} = Z$$

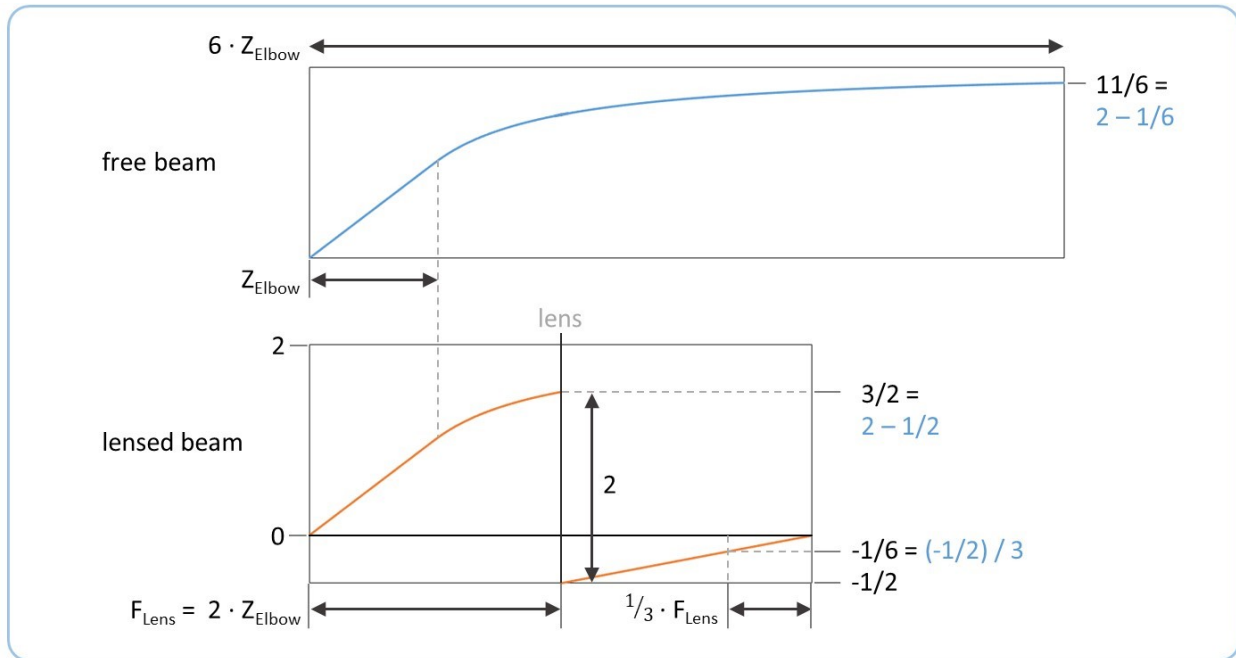
where Z is measured relative to the nearest focal plane. Because both focal planes are the same distance from the lens (except for their opposite signs), the propagation through the flip field is precisely the distance needed to bring the shine to 0.

9.3 Conversion to lensed space

For every plane of a free beam, a corresponding plane can be found in a lensed system. The pattern is identical except for a scale factor; this is trivial in the case of the beam, but significant for a grating or other pattern. The inclinations of the two planes differ by exactly 2 radians.

Figure 9.3 shows how the inclination corresponds between planes. In this example the free beam propagates to a plane at $6x$ the elbow, so the glow impurity or remaining provolution (the distance below the asymptotic inclination of 2) falls to $1/6$.

Figure 9.3, Inclination in free beam vs lensed beam



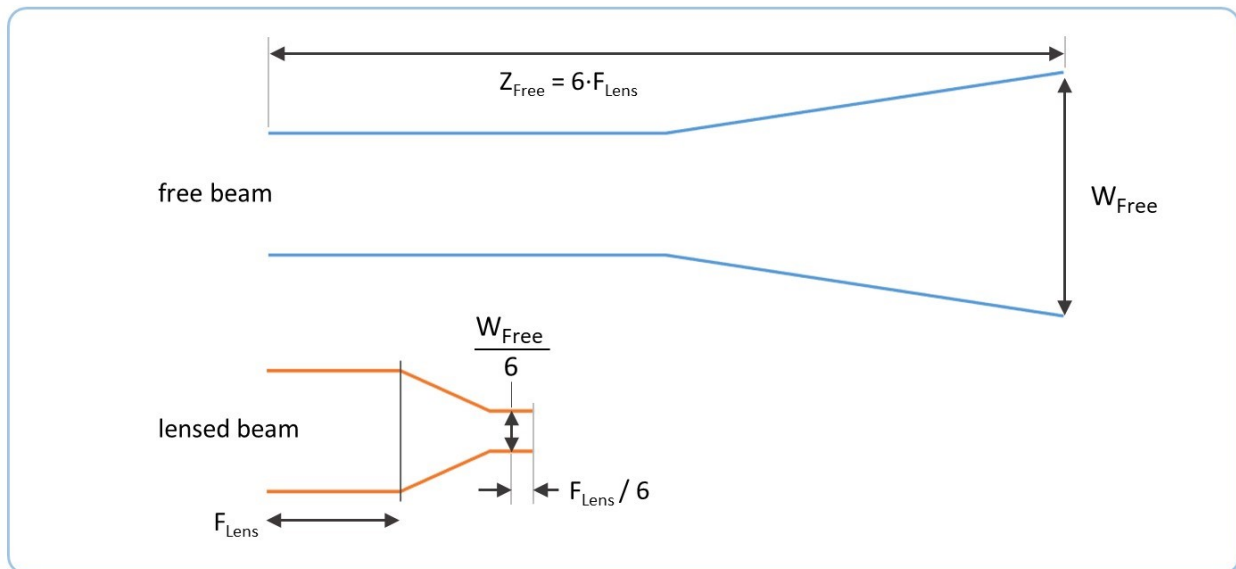
When a similar beam is passed through a lens with $F_{\text{Lens}} = 2 \cdot Z_{\text{Elbow}}$, the glow impurity falls to $1/2$ (inclination $3/2$) before entering the lens. The lens exchanges glow and shine, shifting the inclination by 2 and leaving the beam at an inclination of $-1/2$.

After the lens plane, impurity changes differently in the two systems. In the free beam, it is driven by the growth of shine in the denominator. In the lensed beam, it is driven by the decrease of shine in the numerator. Accordingly, in the free beam the distance from the flat increases by a factor of 3 ($3 \cdot Z_{\text{Lens}} = 6 \cdot Z_{\text{Elbow}}$); in the lensed beam the distance to the *rear* focal plane *decreases* by a factor of 3.

While different-sized beams may undergo different amounts of provolution before the lens, the provolution in the flip field is always exactly the right amount to bring the total provolution to 2 radians, a complete FT. But because of the jump of -2 radians caused by the lens, the final inclination is 0, i.e. the glow is wide and the shine is deep.

A similar correspondence exists for magnification. Figure 9.4 shows the width of the free beam W_{Free} in the plane at 6 times the focal length. When an identical beam passes through a lens, the corresponding plane is demagnified by a factor of 6. As in the previous example, the plane is located at $F_{\text{Lens}}/6$ from the rear focal plane.

Figure 9.4, Magnification in lensed space



10 References

1. Mirsky, Paul L. A First Look at Feature Optics. <http://vixra.org/abs/1909.0157>, 2019
2. Mirsky, Paul L. Feature Optics and the Critical Planes of the Grating. <http://vixra.org/abs/1909.0185>, 2019
3. Mirsky, Paul L. Symmetry and Asymmetry in Feature Optics. <http://vixra.org/abs/1909.0184>, 2019
4. Mirsky, Paul L. Glow and Shine in Feature Optics. <http://vixra.org/abs/2005.0205>, 2020
5. Ozaktas, H.M. and Mendlovic, David. Fractional Fourier transform as a tool for analyzing beam propagation and spherical mirror resonators. Optics Letters, Vol. 19, No. 21, 1994
6. Ozaktas, H.M. and Mendlovic, David. Fractional Fourier Optics, J. Opt. Soc. Am. A, Vol. 12, No. 4, April 1995

7. Ozaktas, H.M., Zalevsky, Zeev, and Kutay, M. Alper. The Fractional Fourier Transform with Applications in Optics and Signal Processing. Wiley and Sons, 2001
8. Saleh, B.E.A. and Teich, M.C., Fundamentals of Photonics, 2nd Edition, Wiley-Interscience, 2007